High Frequency Properties and Applications of Carbon Nanotube (CNT)

Hao Xin

ECE Dept. & Physics Dept.

University of Arizona

Outline

- Introduction and motivation
- Microwave VNA characterization
- THz time domain free space measurement
- Conclusion

MMW Millimeter Wave Circuits and Antennas Laboratory

Our research focus on microwave / mmW / THz antennas, circuits and applications
Capabilities including: Complete Design / Simulation / Fabrication / Characterization

http://ece.arizona.edu/~mwca/

Research Areas

- Novel Electronically Scanned Antennas
- Meta-material for mmW applications
- Nano Devices and Antennas
- Novel THz Sources and Components
- Monolithic Microwave IC (MMIC)
- 3-D Integrated mmW Circuits and Antennas
- Power Harvesting Applications
- Biological Inspired Direction Finding

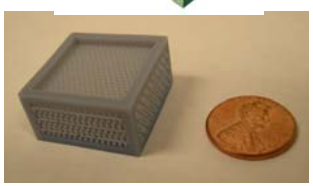

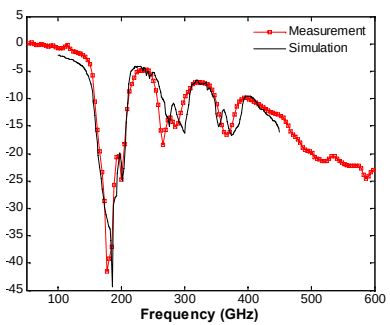

3-D THz Rapid Component Fabrication

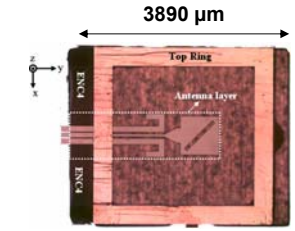

60 GHz Packaged Antenna
Fully Compatible with Si RFIC

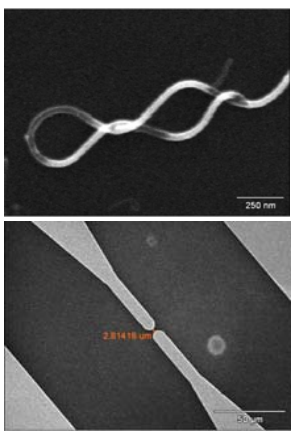

High Frequency Carbon Nanotube Research

Novel Electronic-Scanned Array

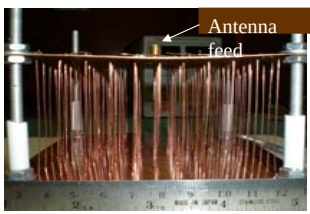

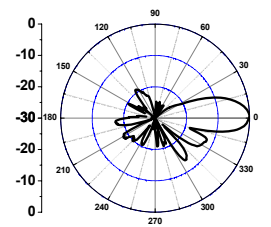

Metamaterial Based Antennas

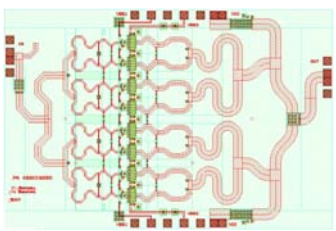

Power Amplifier MMIC

Prof. Hao Xin
hxin@ece.arizona.edu
520-626-6941

National Science Foundation
WHERE DISCOVERIES BEGIN

ARO

US Air Force

DARPA

U.S. ARMY

Raytheon

DoE

TELEDYNE SCIENTIFIC & IMAGING
A Teledyne Technologies Company

Testing Facilities

- Complete microwave to THz characterization facilities
  - Network analyzers (up to 110 GHz), THz equipments
  - Semiconductor parametric analyzer
  - Spectrum analyzer, signal generators, power meters, noise figure meter, etc.
  - Wafer probe station, antenna anechoic chamber

Agilent E8361A Network Analyzer
10 MHz to 67 GHz, 1.85mm test ports
various coaxial and waveguide cal kits

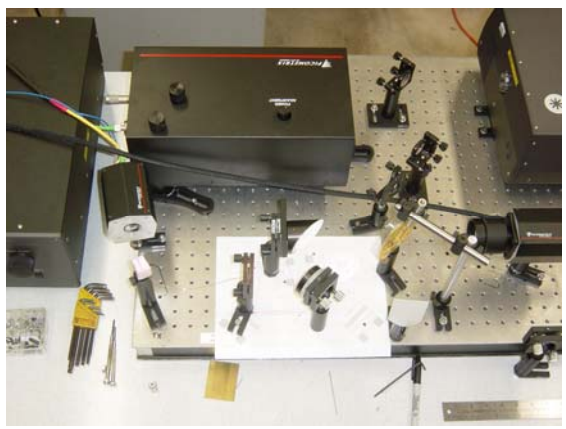

Time Domain THz Spectrometer
(TDS) 50 GHz – 2 THz

Probe Station with various probe
Positioners DC to millimeter probes
and calibration substrates

Fabrication Facilities

- Full capability clean rooms at engineering and optical science (a brand new SEM & NPGS)
- In-house CVD system for nanotube growth
- In-house PCB fabrication equipment

Evaporator
Sputter
E-Beam Lithography
Mask Aligner

Dry Film PCB Fabrication Equipment

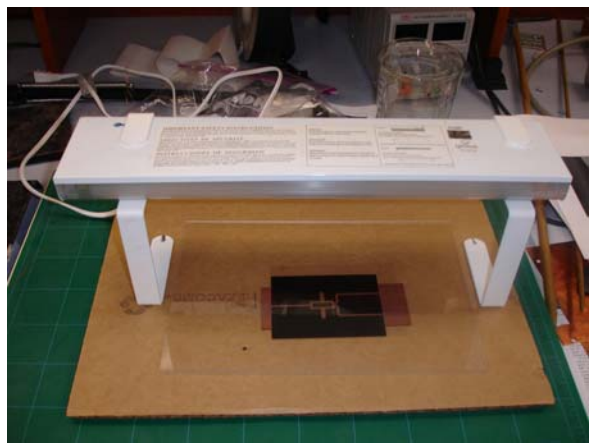

Chemical Vapor Deposition System For Carbon Nanotube Growth

- Access of semiconductor foundries
  - Raytheon RRFC / Teledyne Scientific Company / MIT Lincoln Laboratory (GaAs, InP, and CMOS)

Modeling / Simulation Capabilities

- Advanced electromagnetic and circuit simulation tools
  - Linear / Non-linear circuit simulators
  - Finite-element frequency domain and time domain simulators
  - Agilent Advanced Design Systems, Momentum, **HFSS, CST, SEMCAD++,** Cadence, Sonnet …
  - Work Stations with 12 GB RAM
  - Evaluating parallel EM simulation tools such as **GEMS**

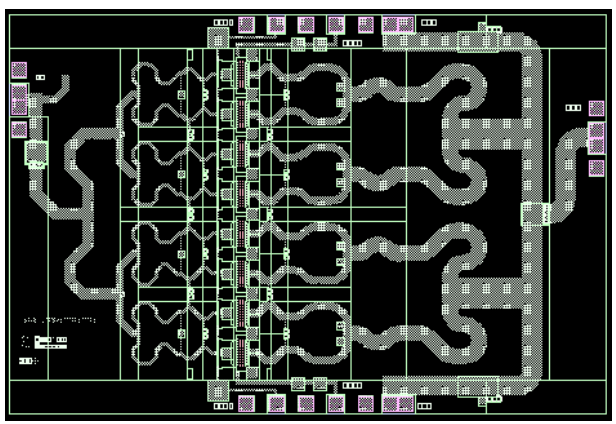

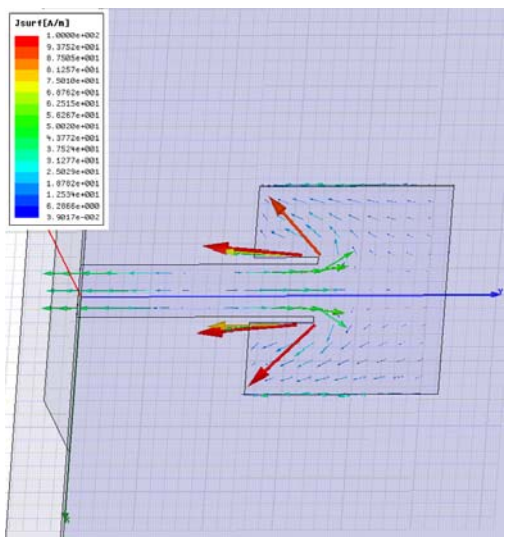

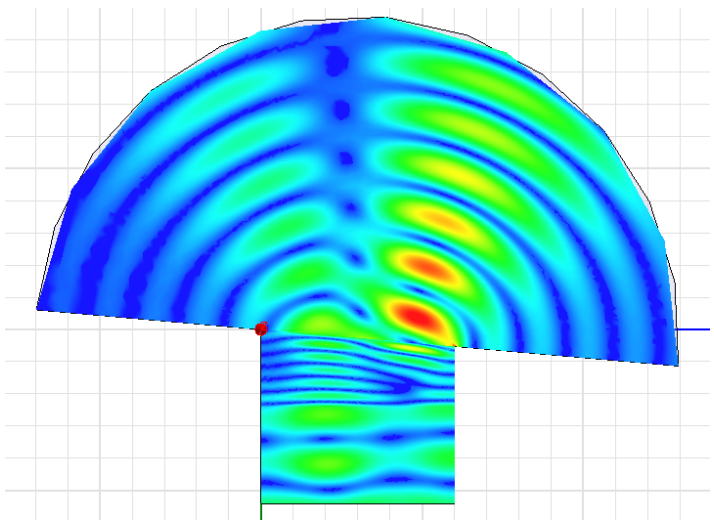

Background and Motivation

❑ Carbon Nanotube (CNT) (Diameter ~ nm)

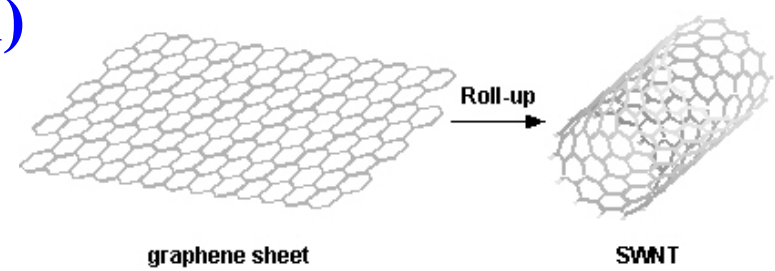

- Discovered by S. Lijima in 1991
- Rolled-up sheet(s) of graphene
- Metallic CNT can have current density 1000 times greater than metals (> 10^9 A/cm^2 vs. < 10^7 A/cm^2 for Cu)
- One of strongest and stiffest materials

❑ SWNT (Single-Walled)

- Chirality => Semconducting or metallic
- Bandgap can be tuned by the chirality of SWNT

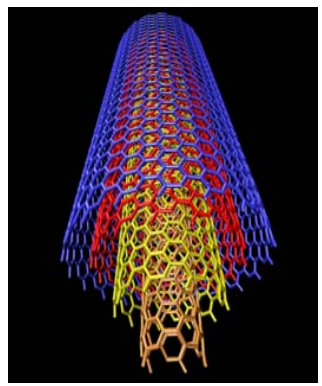

3-D structure of MWNT

❑ MWNT (Multi-Walled)

- Multi-layers in parallel => Tend to be metallic

❑ Main technology issue: material control / fabrication

Images are taken from www.nanotech-now.com

Structure and properties of SWNT

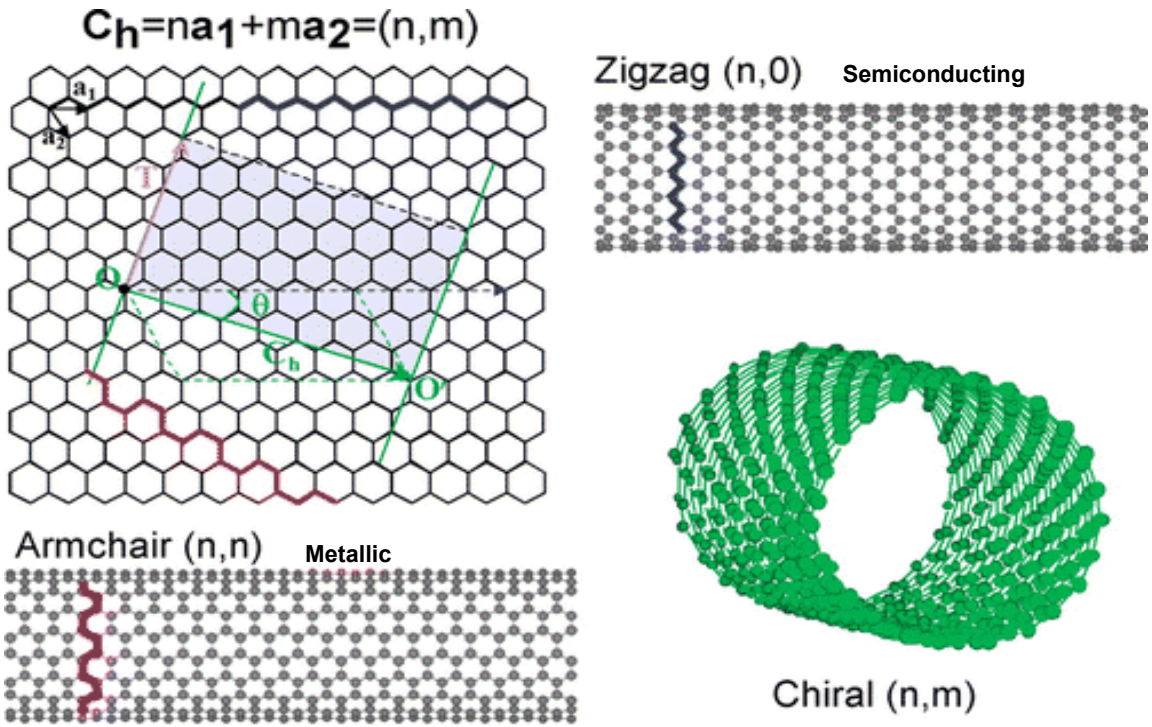

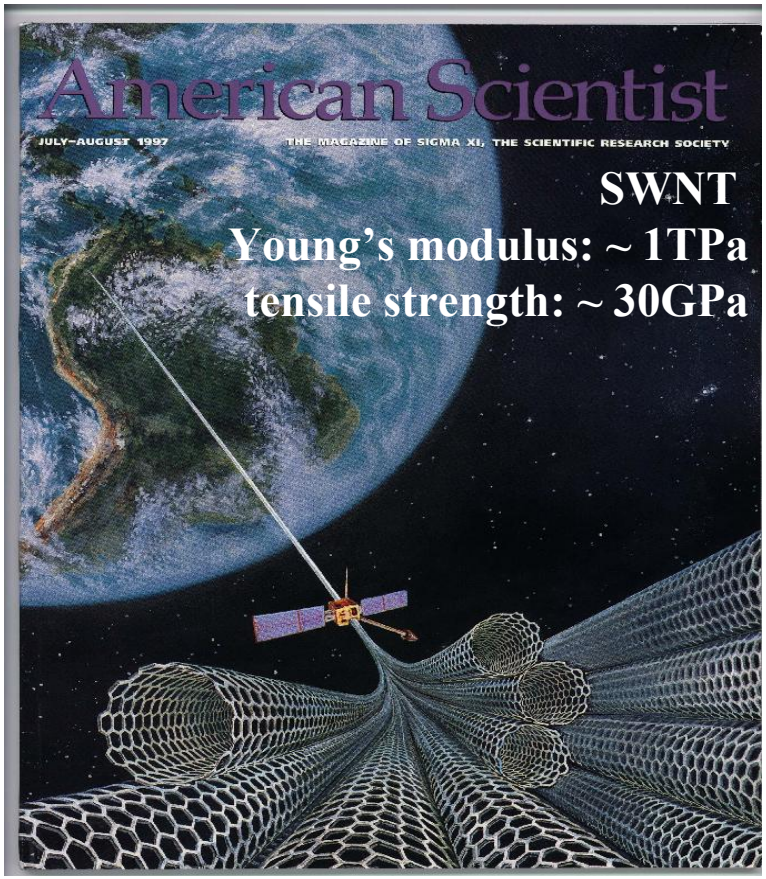

Lieber et.al. ***J. Phys. Chem. B*** 104, 2794-2809 (**2000**)

- **Semiconducting SWNT – active devices**
- **Metallic SWNT – passive interconnects**
- **Possibly: all carbon IC**

Potential High Frequency Applications: GHz - THz

❑ Field Effect Transistors

- **Significant better device performance metric[1]**
- **Up to THz intrinsic cutoff frequency predicted[2]**

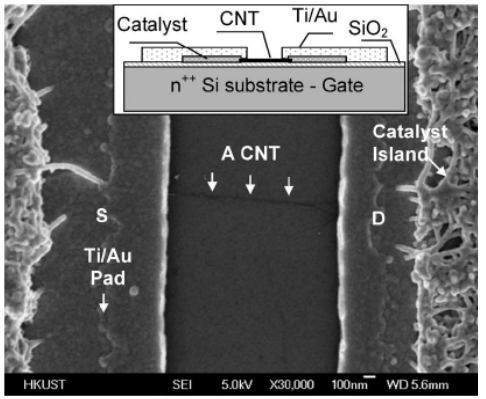

❑ Passive Applications: Interconnect, Antenna

- Transmission line model of CNTs
- Quantum / Kinetic inductance (~ 10,000 higher than magnetic inductance)
- Resonance frequency 100 times lower ($\sim\sqrt{1/LC}$): much smaller antenna

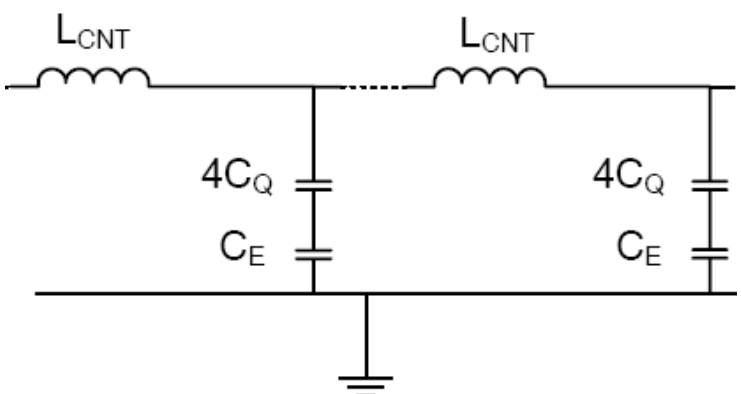

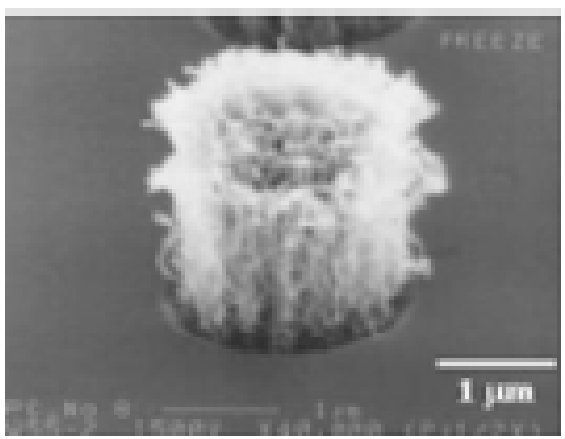

1. J. Guo et al, IEDM, pp. 711 (2002)

2. P. J. Burke, Solid-StateElectron., 40, 1981, (2004)

High-frequency measurement of CNT

❑ Challenge of Single-tube measurement

- Significant mismatch between single CNT's high intrinsic impedance and 50Ω microwave testing system
- Parasitics often dominate the intrinsic CNT properties
- Difficulty of test fixture fabrication
- Kinetic inductance at microwave frequency has not been experimentally verified

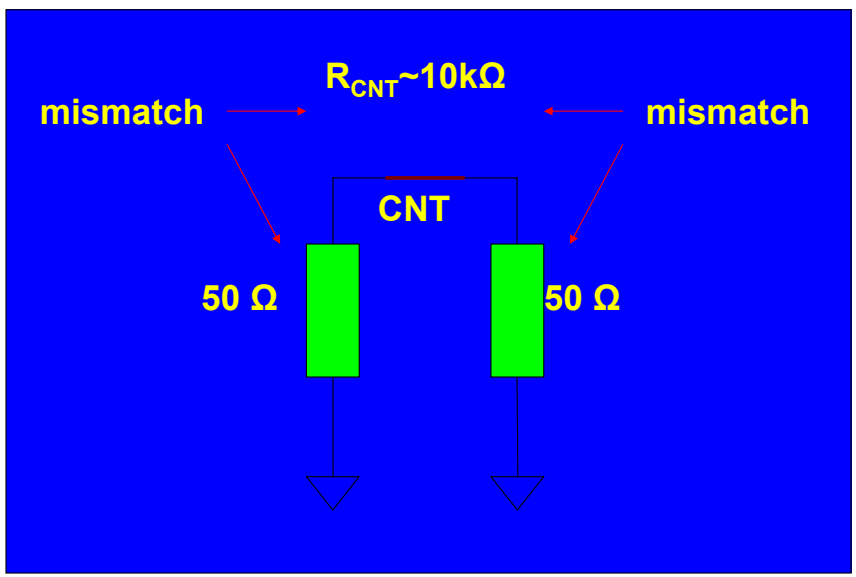

A CNT across electrodes using Electrophoresis

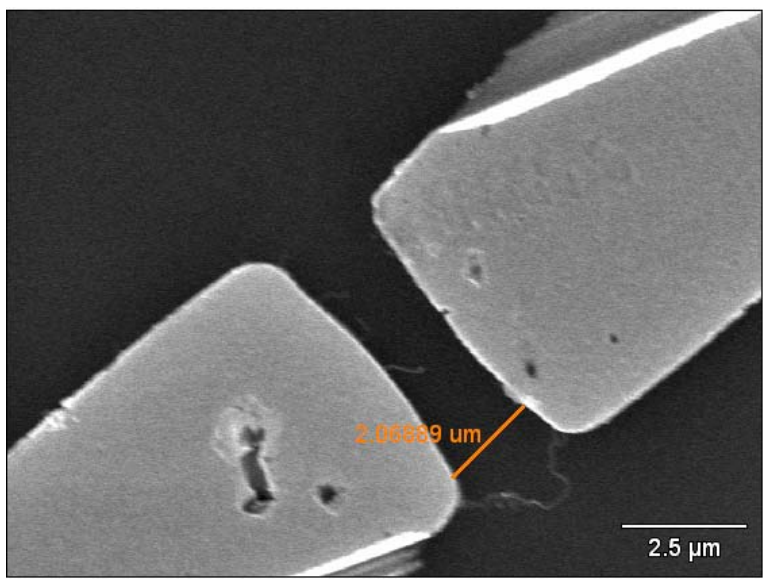

Alternative Measurement Approach

❑ **Alternative approach: measure an ensemble of CNTs (CNT paper, array etc.) and extract intrinsic properties**

➢ **May be necessary for practical applications (bundles, thin film devices, etc. are currently more promising)**

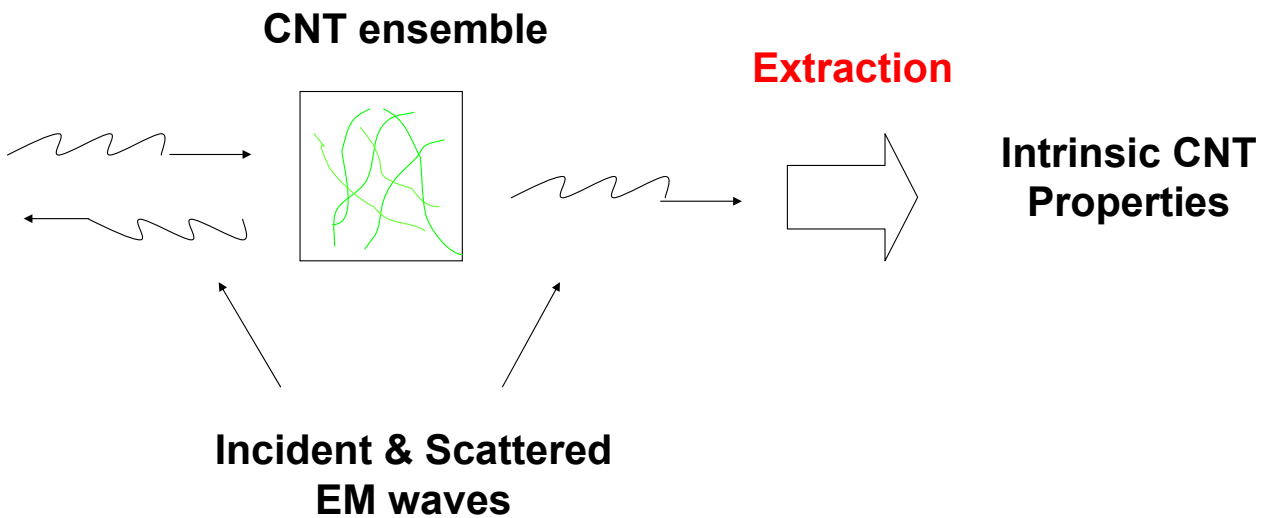

Characterization of CNT Ensembles

- **Limitation of reported CNT ensemble measurements**
  - Measured only transmission or reflection
  - The assumption of μ=1 had to be made
  - Lack of error analysis
- **Goal: Study high frequency properties of CNTs**
  - Vector Network Analyzer (10 MHz – 110 GHz)
  - THz Time Domain Spectrometer (50 GHz – 3 THz)
  - Characterization of both SWNT and MWNT

MWNT Paper Sample

- Thickness: 3.5 mil (~90 μm)
- MWNTs are randomly oriented

Preparation

Suspend MWNTs in a fluid

Filter the fluid onto a membrane Support

Dry the membrane and remove the MWNT paper

MWNT paper photo

SEM image

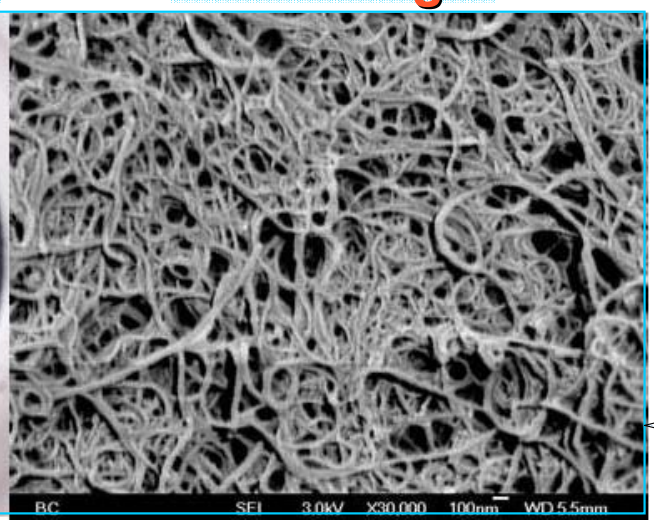

VNA Experimental Setup

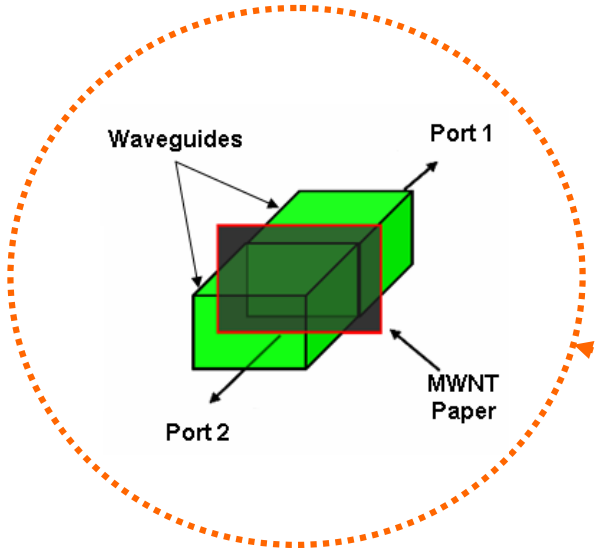

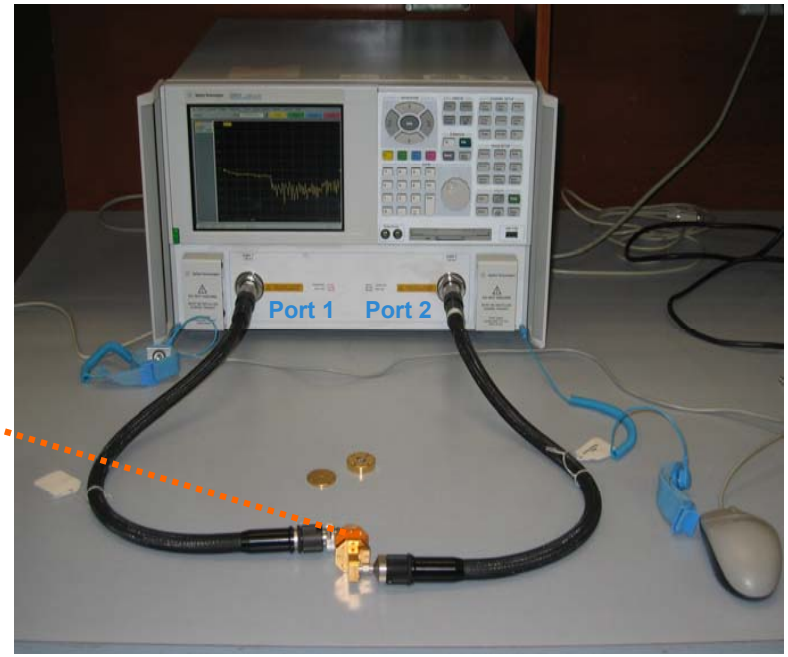

- Characterized with state-of-art Agilent E8361A PNA network analyzer (10MHz-67GHz)
- Calibrated with waveguide cal kit before measurement
- MWNT paper sandwiched between two rectangular waveguides
- Both of magnitudes and phases of reflection (S11) and transmission (S21) are measured

Extracting Intrinsic Material Properties

- Nicolson-Ross-Weir (NRW)

approach is implemented

- m=0 is selected and verified

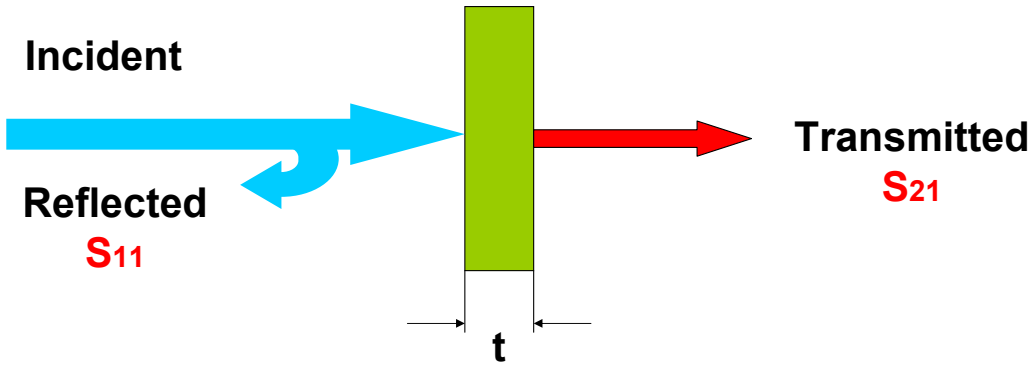

- $\varepsilon = \varepsilon' - j\,\varepsilon''$ and $\mu = \mu' - j\,\mu''$ are complex permittivity and permeability normalized to free space.

$$V_1 = S_{21} + S_{11}$$
$$V_2 = S_{21} - S_{11}$$

$$X = \frac{1 + V_1 V_2}{V_1 + V_2}$$

$$\xi = X \pm \sqrt{X^2 - 1}$$

$$\Gamma = \frac{\xi - V_2}{1 - \xi V_2}$$

$$\mu = \frac{\eta' Z_{pv}^r}{k_0 t}[\,j \ln|\xi| - (\theta + 2m\pi)]$$

$$\varepsilon = \frac{\mu}{\eta'^2 Z_{pv}^{r\ 2}}$$

Extracted Permittivity and Permeability

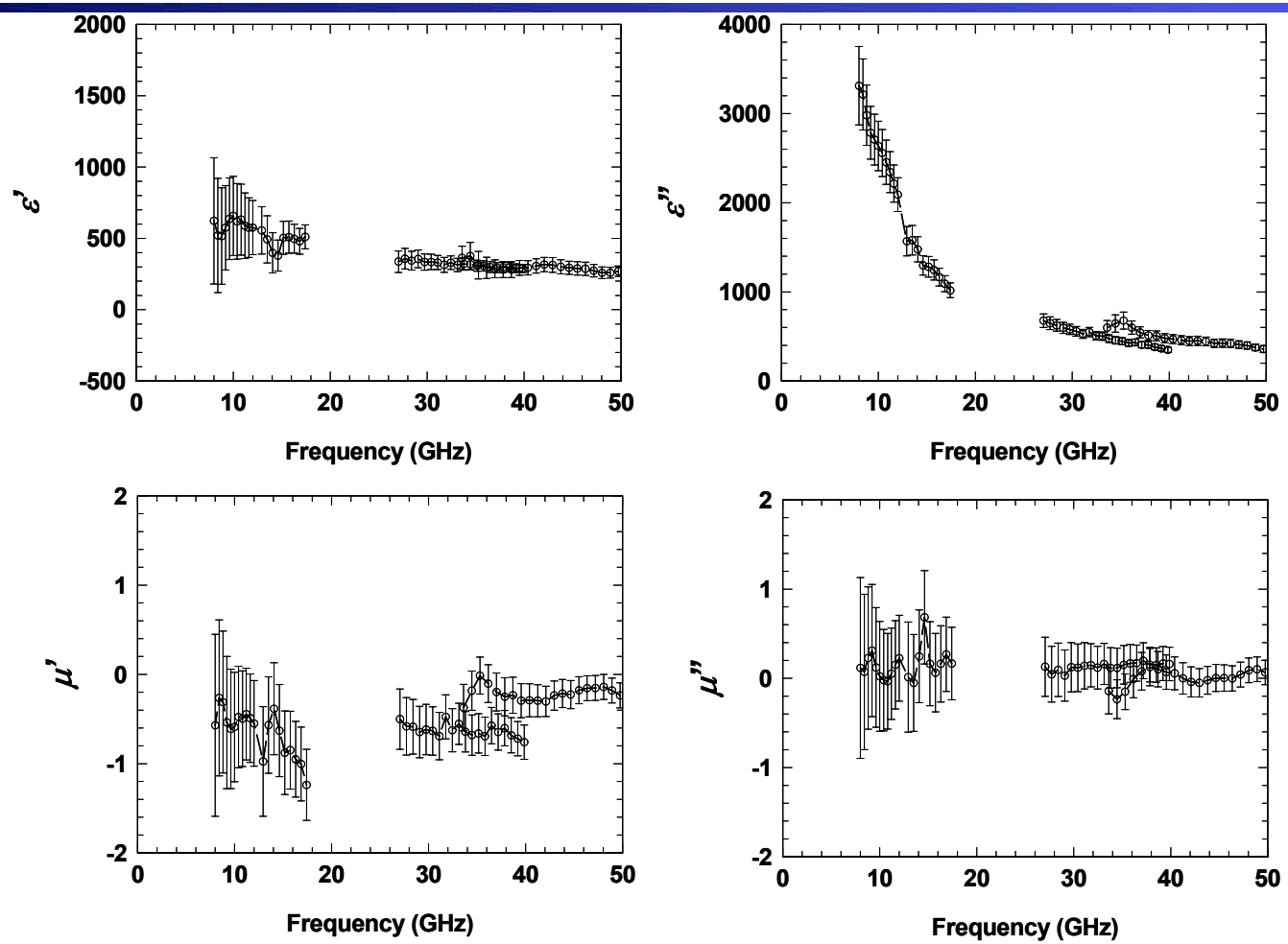

- Resulting conductivity $\sigma=\varepsilon''\omega\varepsilon_0$ ~ 1500 S/m, close to DC conductivity 1000 S/m
- No significant magnetic response
- Negative μ'' are due to numerical spill over from ε''

1. L. Wang, R. Zhou, and H. Xin, IEEE Trans. Microwave Theory and Tech., Vo. 56, No. 2, pp. 499-506, February, 2008

Verification of the Algorithm

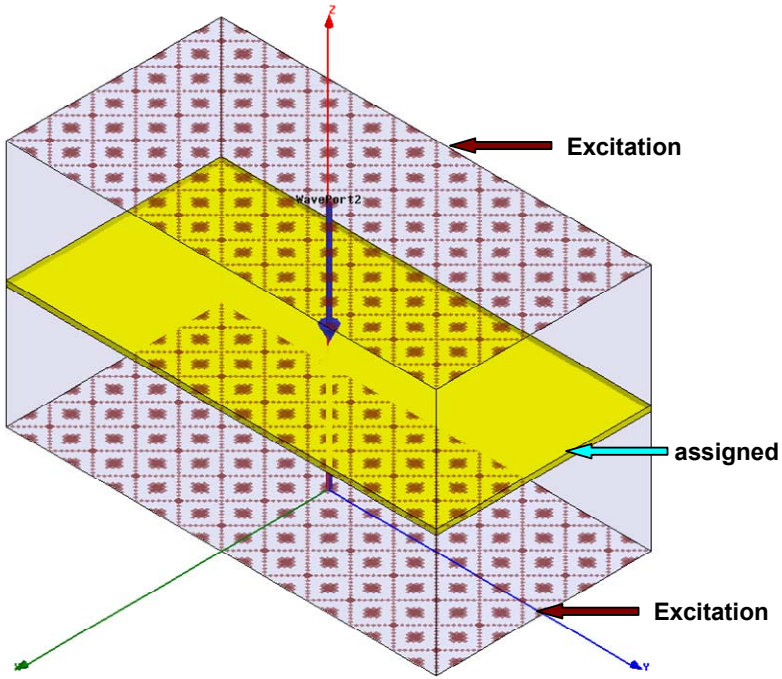

HFSS simulation Model

Ansoft's HFSS (High Frequency Structure Simulator) is employed for simulation.

- A 3.5-mil thin slab is assigned with extracted ε and μ and sandwiched between two waveguides
- The simulated S-parameters are consistent with measured S-parameters

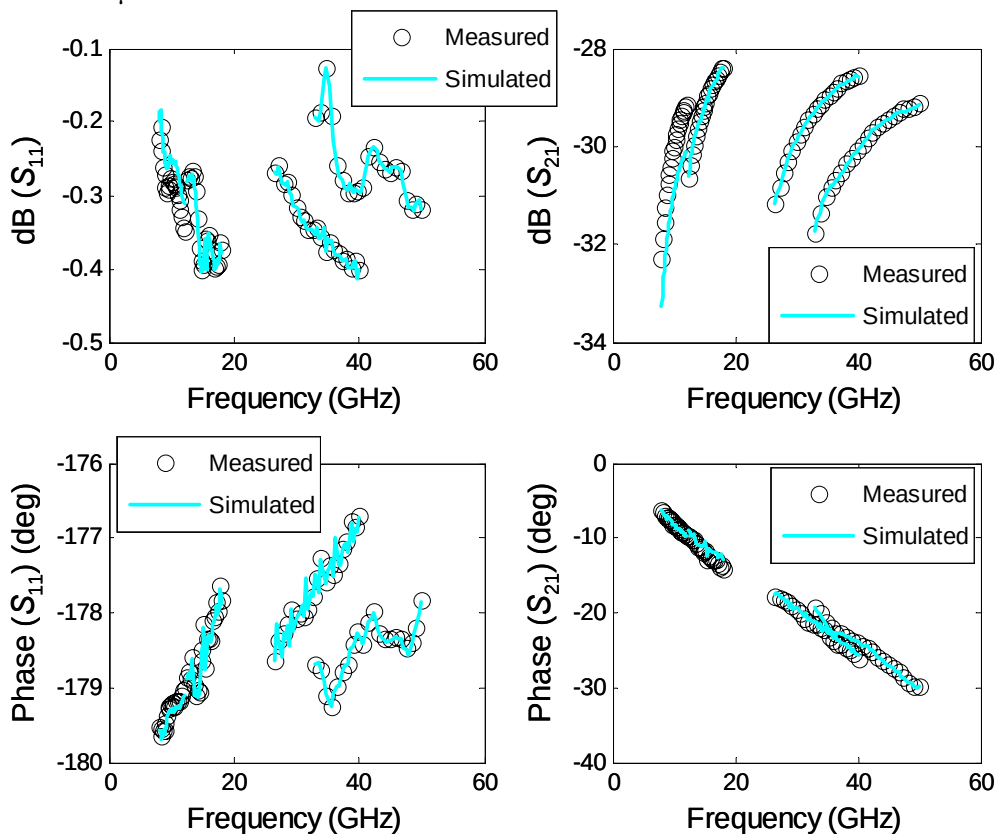

Error Analysis

$$\Delta\varepsilon' = \sqrt{(\frac{\partial\varepsilon'}{\partial|S11|}\Delta|S11|)^2 + (\frac{\partial\varepsilon'}{\partial\angle S11}\Delta\angle S11)^2 + (\frac{\partial\varepsilon'}{\partial|S21|}\Delta|S21|)^2 + (\frac{\partial\varepsilon'}{\partial\angle S21}\Delta\angle S21)^2}$$

$$\Delta\varepsilon'' = \sqrt{(\frac{\partial\varepsilon''}{\partial|S11|}\Delta|S11|)^2 + (\frac{\partial\varepsilon''}{\partial\angle S11}\Delta\angle S11)^2 + (\frac{\partial\varepsilon''}{\partial|S21|}\Delta|S21|)^2 + (\frac{\partial\varepsilon''}{\partial\angle S21}\Delta\angle S21)^2}$$

$$\Delta\mu' = \sqrt{(\frac{\partial\mu'}{\partial|S11|}\Delta|S11|)^2 + (\frac{\partial\mu'}{\partial\angle S11}\Delta\angle S11)^2 + (\frac{\partial\mu'}{\partial|S21|}\Delta|S21|)^2 + (\frac{\partial\mu'}{\partial\angle S21}\Delta\angle S21)^2}$$

$$\Delta\mu'' = \sqrt{(\frac{\partial\mu''}{\partial|S11|}\Delta|S11|)^2 + (\frac{\partial\mu''}{\partial\angle S11}\Delta\angle S11)^2 + (\frac{\partial\mu''}{\partial|S21|}\Delta|S21|)^2 + (\frac{\partial\mu''}{\partial\angle S21}\Delta\angle S21)^2}$$

- The partial derivatives are computed numerically. For example, to calculate $\partial\varepsilon'/\partial|S11|$, we evaluate ε' with $|S11|+\delta$ while all other parameters remaining the same (δ: small number, selected to be 1E-4), then $\partial\varepsilon'/\partial|S11| = [\varepsilon'(|S11|+\delta) - \varepsilon'(|S11|)]/\delta$. The S-parameters uncertainties are provided by Agilent.

Error Analysis (cont')

- The systematic errors of ε'' (less than +/- 15%) are much smaller than ε', μ' and μ''.
- ε'' extracted from different data sets are fairly close (within +/- 6.5%), but ε', μ' and μ'' change dramatically. Consistent with the above theoretical prediction.
- Overestimation of errors (6.5%<15%) is due to
  - Worst-case S-parameter uncertainties
  - Numerical partial derivative evaluations
- Systematic errors are more sensitive on *S11* uncertainties than *S21* uncertainties. Consistent with expectation.
  - Most of energy is reflected. Change of material properties leads to larger difference on *S21* than *S11*, in other words, little variation in *S11* will cause dramatic change on ε and μ.

Intrinsic Permittivity of MWNT

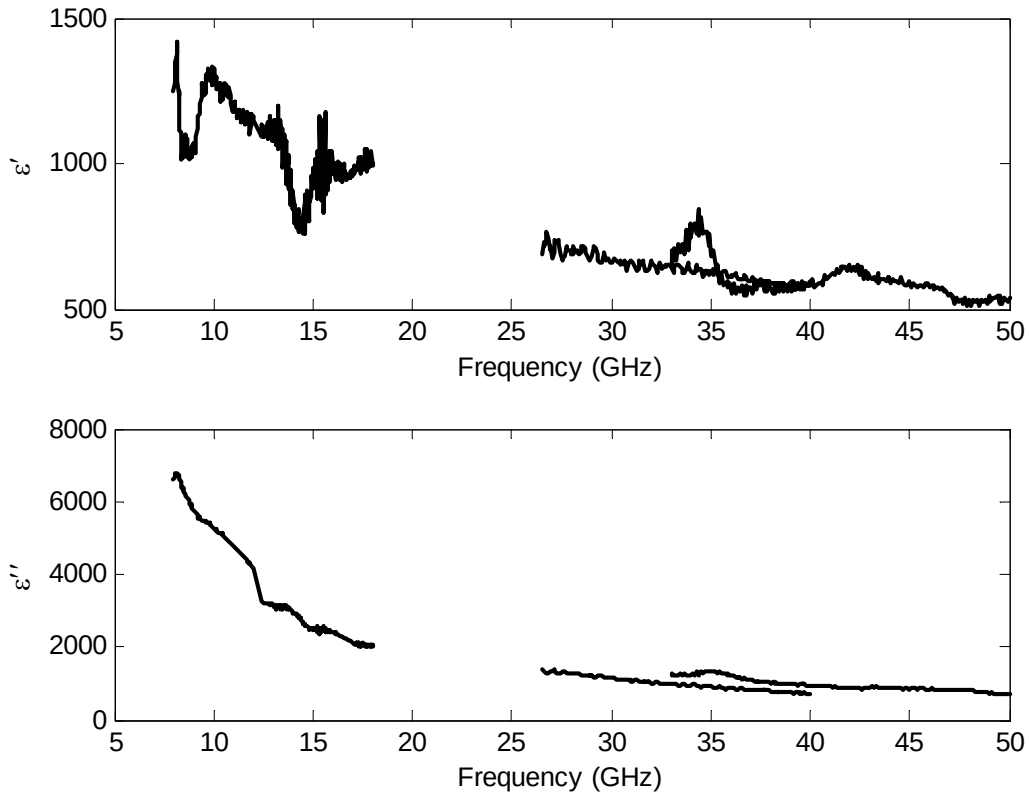

Composite with a & b

$$f_a \frac{\varepsilon_a - \varepsilon_{eff}}{\varepsilon_a + K\varepsilon_{eff}} + f_b \frac{\varepsilon_b - \varepsilon_{eff}}{\varepsilon_b + K\varepsilon_{eff}} = 0$$

$$K = \frac{1-q}{q}$$

f's are volume fractions

$$q = \frac{1/a_2}{1/a_1 + 2/a_2}$$

a's are diameter & length of individual MWNT

- Bruggeman Effective Medium Theory (EMT) applied to remove the effect of air in MWNT paper and extract the intrinsic permittivity of MWNT
- ε' and ε'' are roughly doubled

THz Time Domain Spectrometer (TDS) Setup

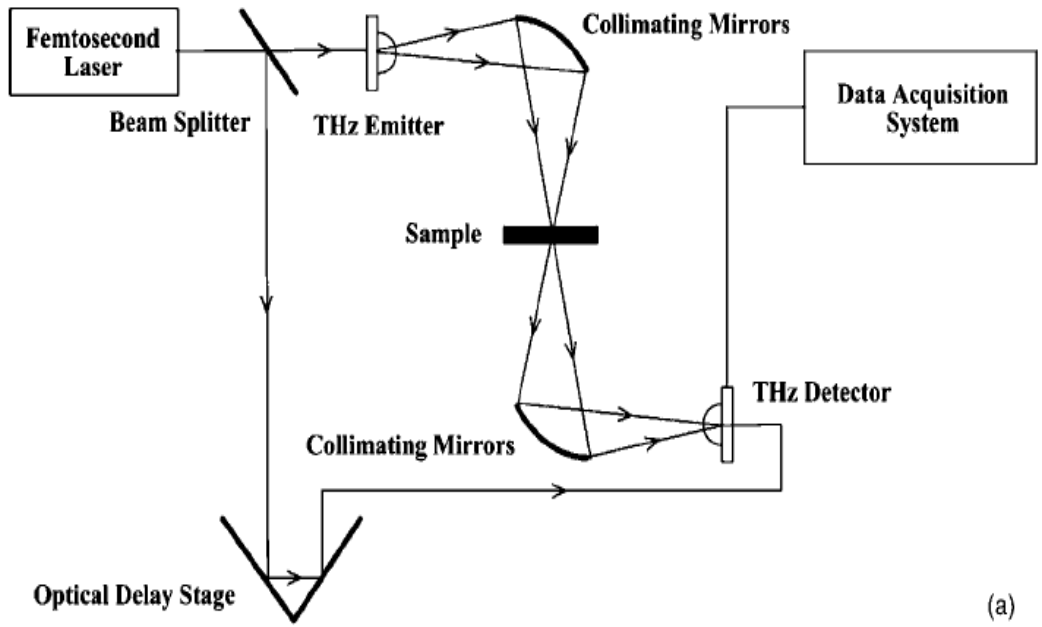

(a)

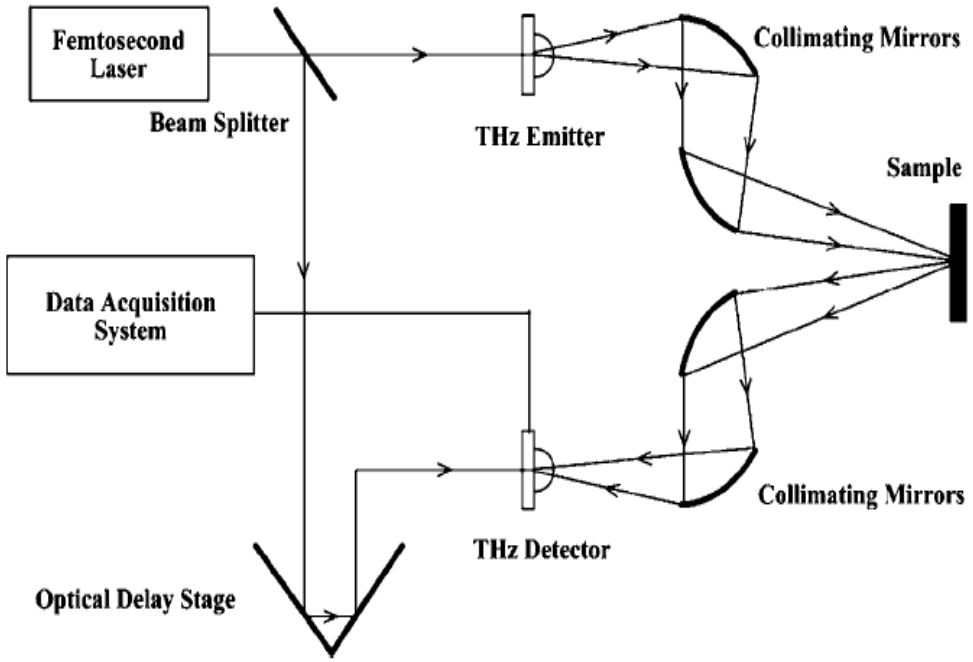

(b)

- Femto-second laser excites a low-temp grown GaAs substrate
- THz pulse generated and transmitted to sample
- Same laser pulse optically delayed to detector: coherent measurement
- Transmission and reflection magnitudes & phases can be measured

1. Z. Wu, L. Wang, A. Young, S. Seraphin, and H. Xin, J. App. Phys., Vol. 103, No. 9, May, 2008 (*This article was also published in the June 2, 2008 issue of the Virtual Journal of Nanoscale Science & Technology (www.vjnano.org)*

Detailed THz Experimental Setup

- Photoconductive THz-TDS system (50GHz-1.5THz)
- Transmission Setup
  - Sample-out as reference spectrum
  - Sample-in as sample spectrum
- Reflection Setup
  - Metal plate as reference object (reflection -1)
  - CNT sample and metal plate surfaces placed at the same position
    (misalignment <12.7 μm)
  - Incidence angle 26°

THz-TDS Results

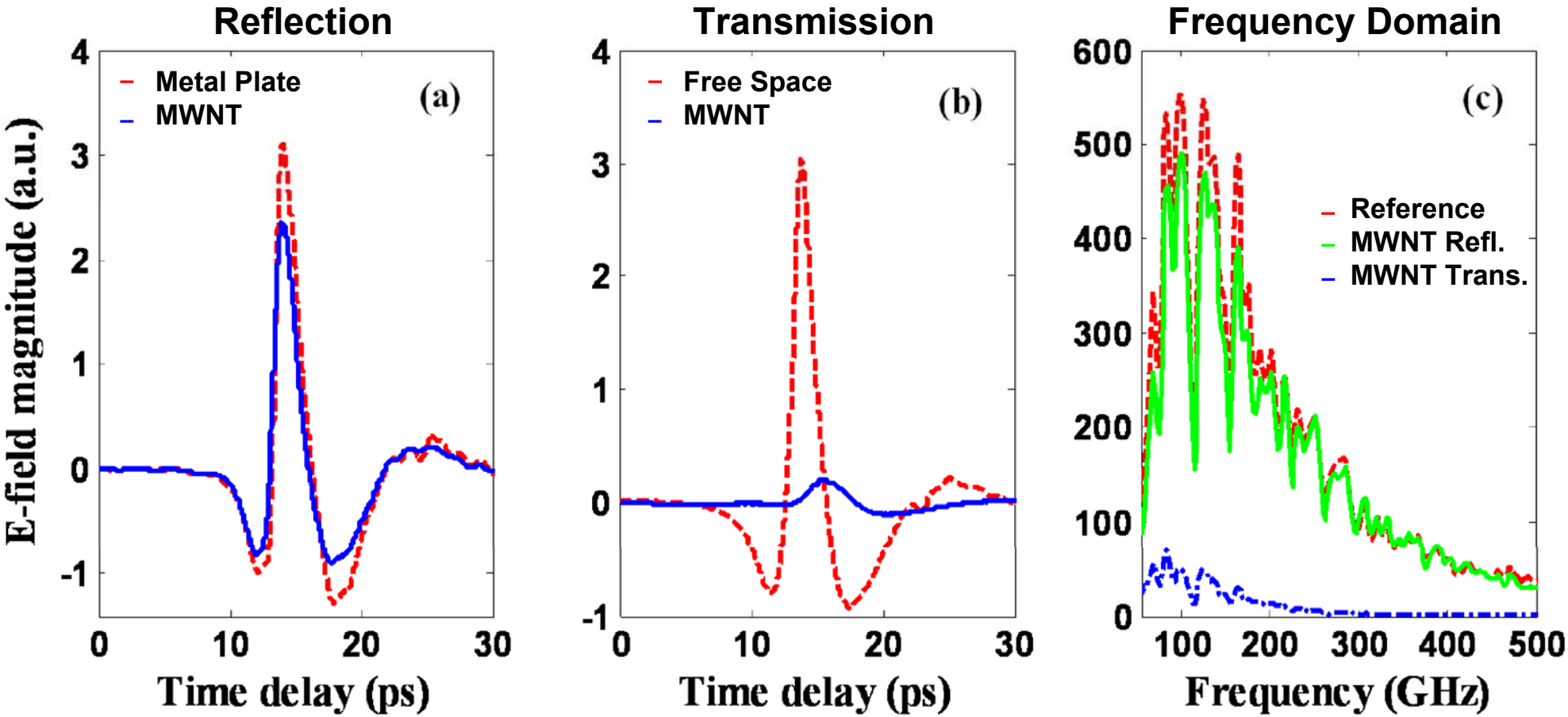

- Large reflection from MWNT sample
- Small transmitted signal through the sample
- Higher order multiple reflections ignored

Material Parameters Extraction Algorithm

- Complex refractive index: $n = n' - jn''$ Wave impedance: $z = z' - jz''$
- Complex permittivity: $\varepsilon = n / z$ Permeability: $\mu = n \cdot z$

- First order complex transmission and reflection coefficients:

$$T_0(n,z) = \frac{4z}{(z+1)^2}\exp(j2\pi(1-n)d/\lambda_0) \qquad R_0(n,z) = \frac{z\cos\theta_i - \sqrt{1-(\sin\theta_i / n)^2}}{z\cos\theta_i + \sqrt{1-(\sin\theta_i / n)^2}}$$

- n and z numerically solved from T_0 and R_0
- No need to assume $n = 1/z$ (or $\mu = 1$)
- If $\theta_i \approx 0°$, z and thus n can be analytically solved from T_0 and R_0

$$R_0(z,\theta_i \approx 0) = \frac{z-1}{z+1} \quad \text{(Normal-incidence approximation)}$$

Multiple-Branch Soultions of Index of Refraction

Multiple branches of *n'* solution due to the phase ambiguity in measured T_0

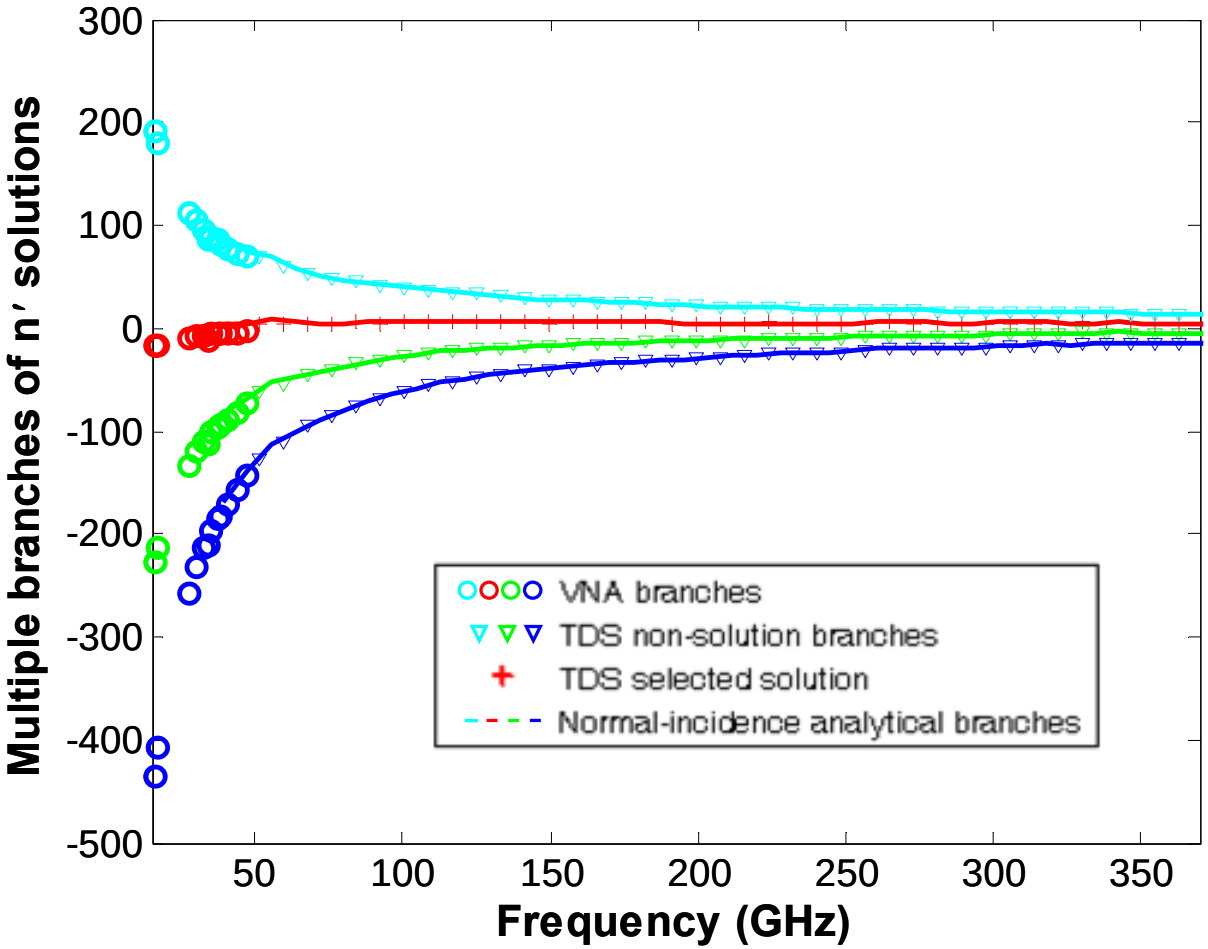

- Good consistency between VNA and TDS measured *n'* solution branches
- Analytically solving n' solutions with $\theta_i \approx 0^\circ$ approximation gets close results

$$n' = 1 - \left(\angle \frac{T_0}{1 - R_0^2} + 2m\pi\right)\frac{\lambda_0}{2\pi d}$$

Extracted n' and n" of MWNT Samples

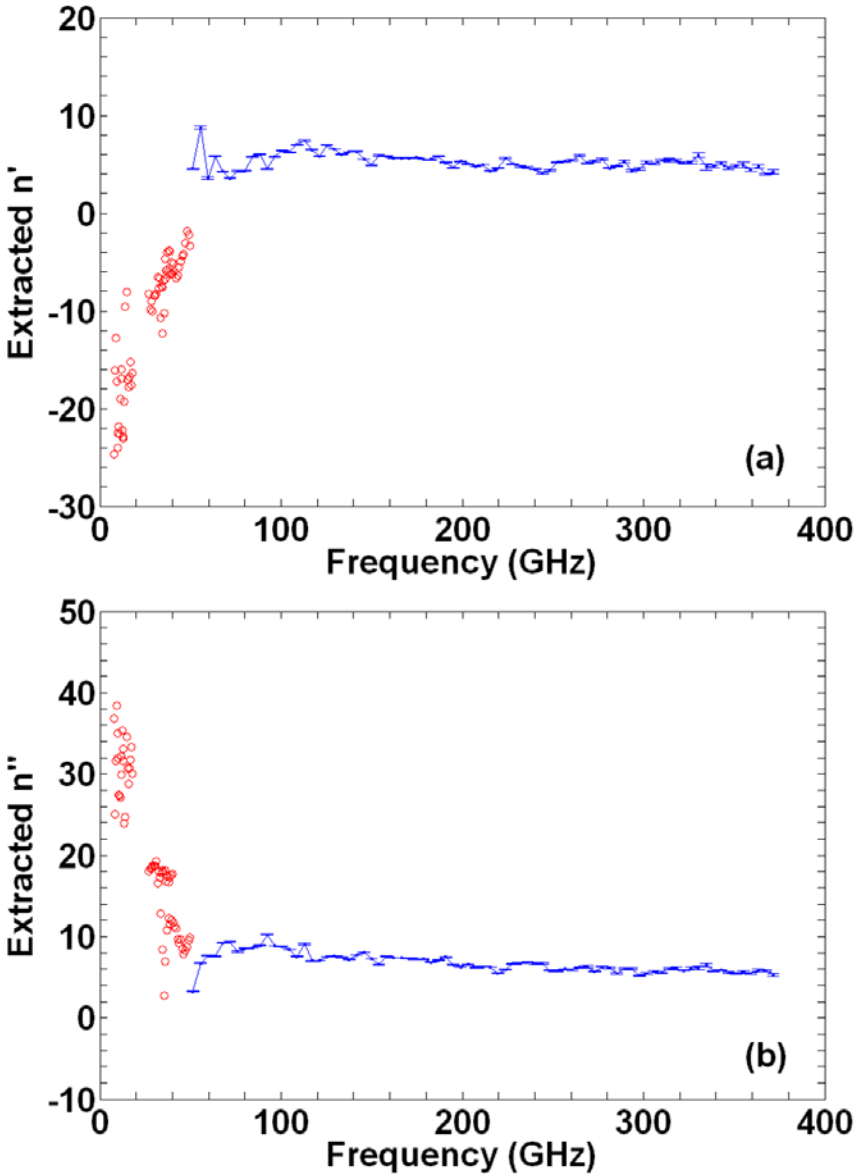

- *m = 0* branch in TDS results is the physically correct branch
- The continuity of *n'* at the boundary frequency is kept
- Good consistency of *n'* and *n"* between VNA and TDS results
- Statistical error bars show good repeatability

Extracted MWNT Permittivity and Permeability

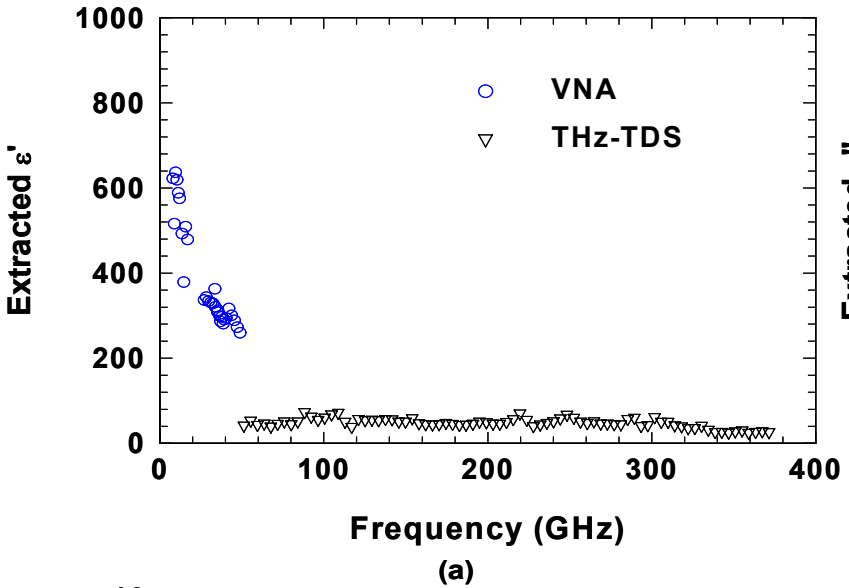

(a)

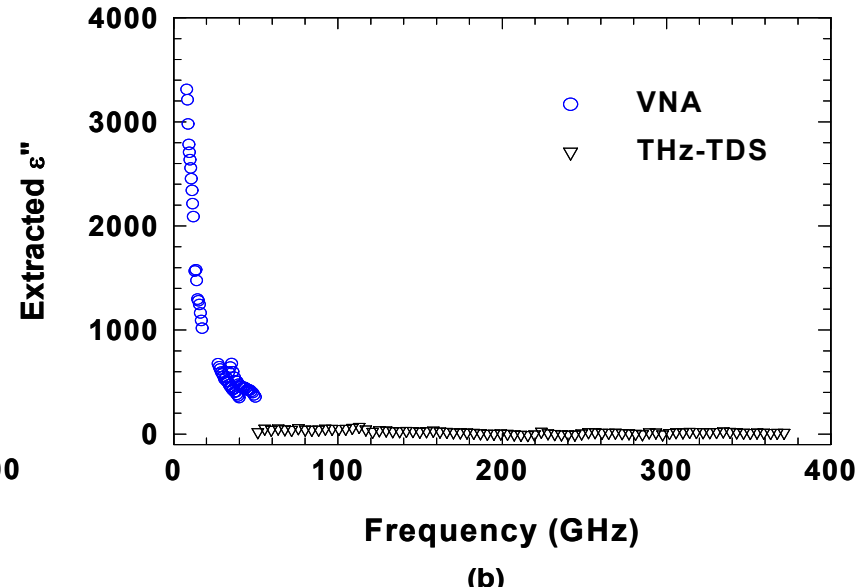

(b)

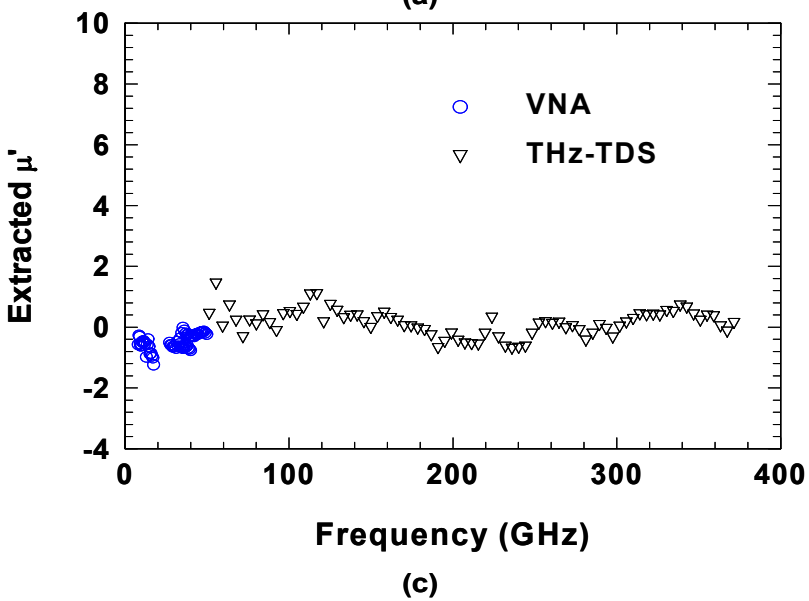

(c)

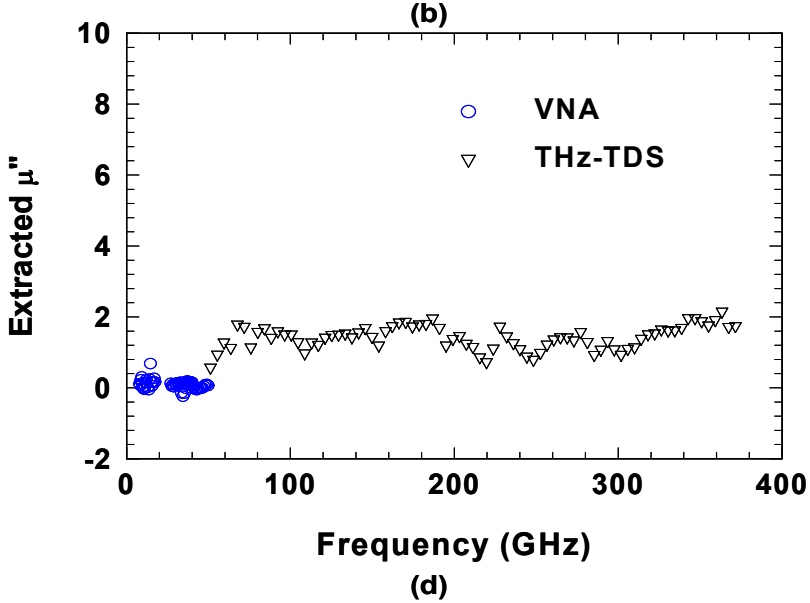

(d)

Drude-Lorentz Model Fitting

$$\varepsilon = \varepsilon_c - \frac{\omega_p^2}{\omega(\omega - i\Gamma)} + \frac{\omega_{p1}^2}{-\omega^2 + i\omega\Gamma_1 + \omega_1^2}$$

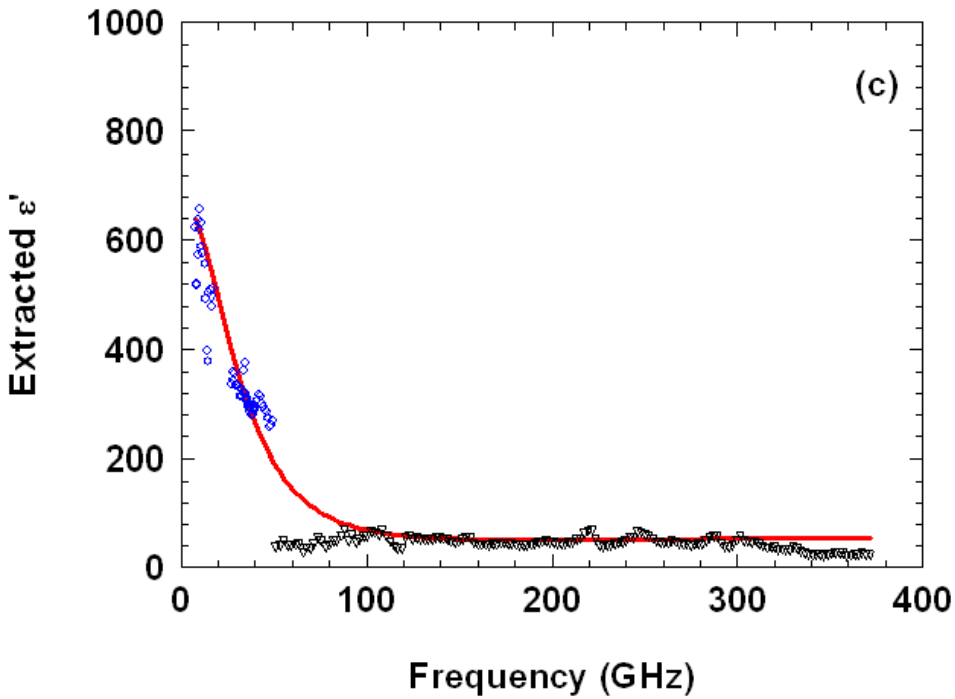

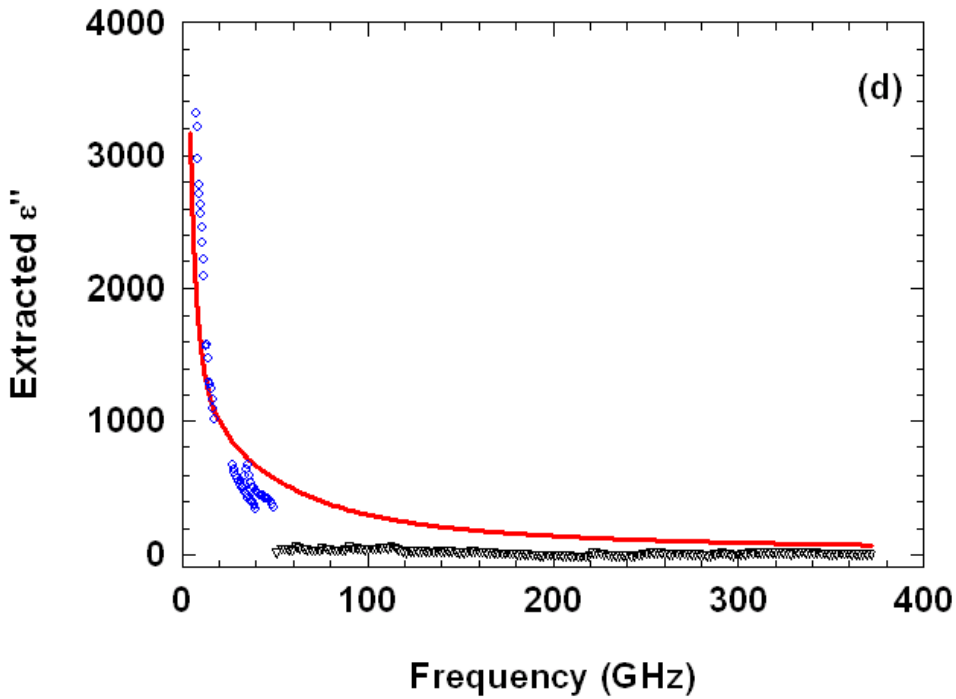

ε_c	ω_p	Γ	ω_{p1}	ω_1	Γ_1
60	7.49×10^{12}	6.46×10^{11}	1.15×10^{14}	4.2×10^{12}	8.1×10^{13}

- ε' and ε'' simultaneously fitted
- Covering microwave to THz

Transmission Measurement Only Evaluation

- With $n = 1/z$ (or $\mu = 1$) assumption:

$$T_0(n,z) = \frac{4n}{(n+1)^2}\exp(j2\pi(1-n)d/\lambda_0)$$

- Solve complex n from T_0

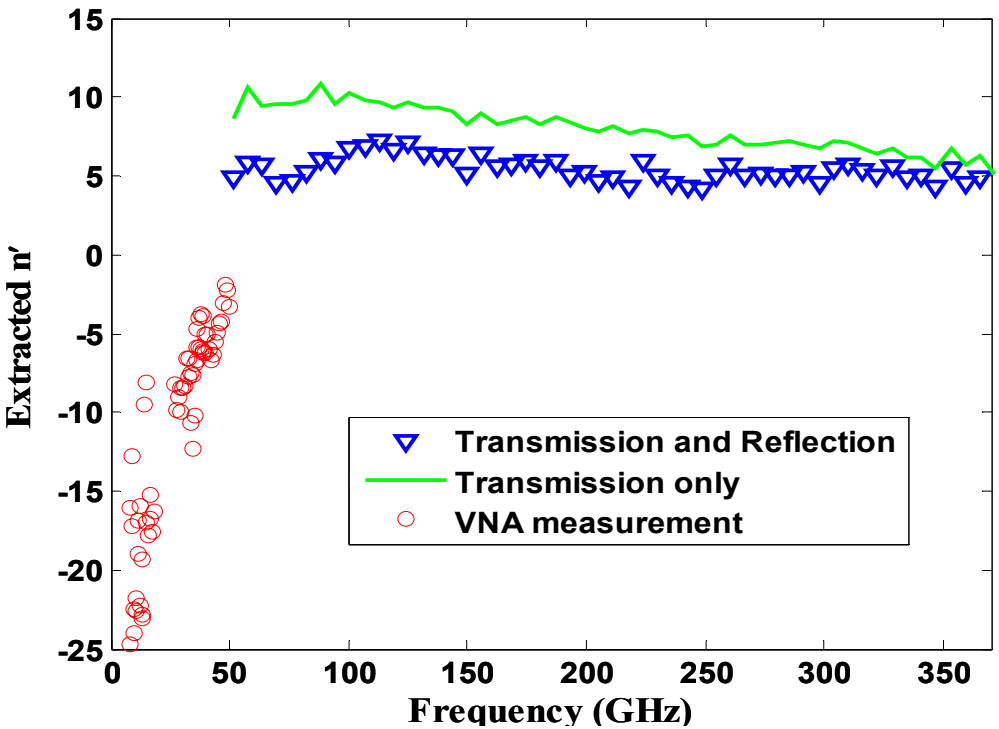

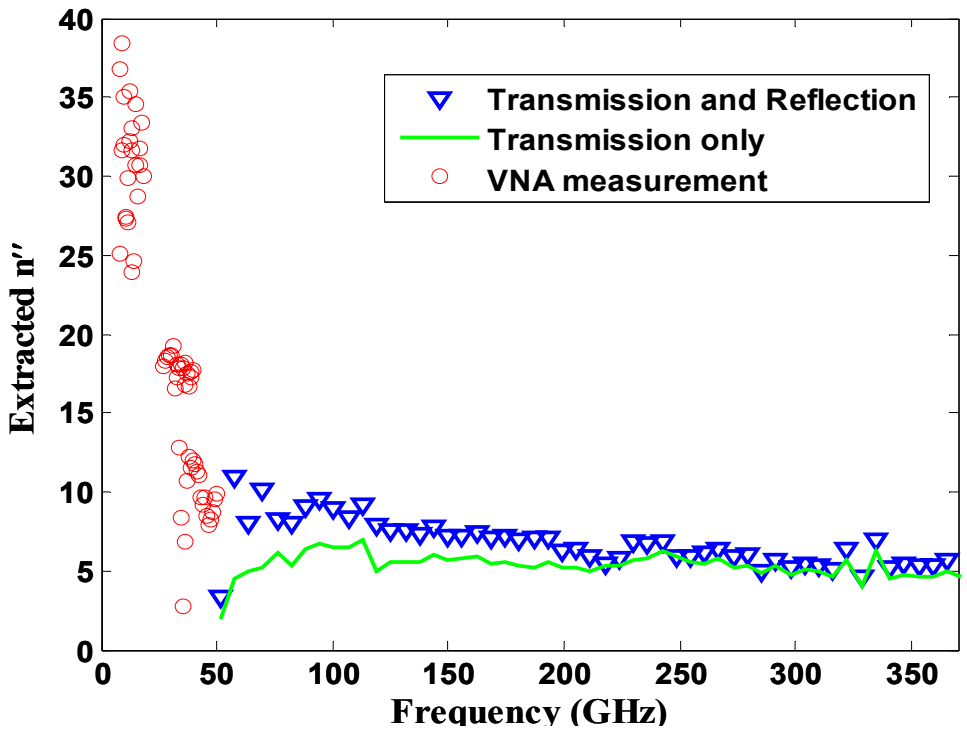

Multiple Reflections Effect in Sample

$$LossFactor = mag\left[\left(\frac{z-1}{z+1}\right)^2 \exp(-4\pi n'' fd/c)\right]$$

Due to one round trip of internal reflections in sample (Transmission/ Reflection)

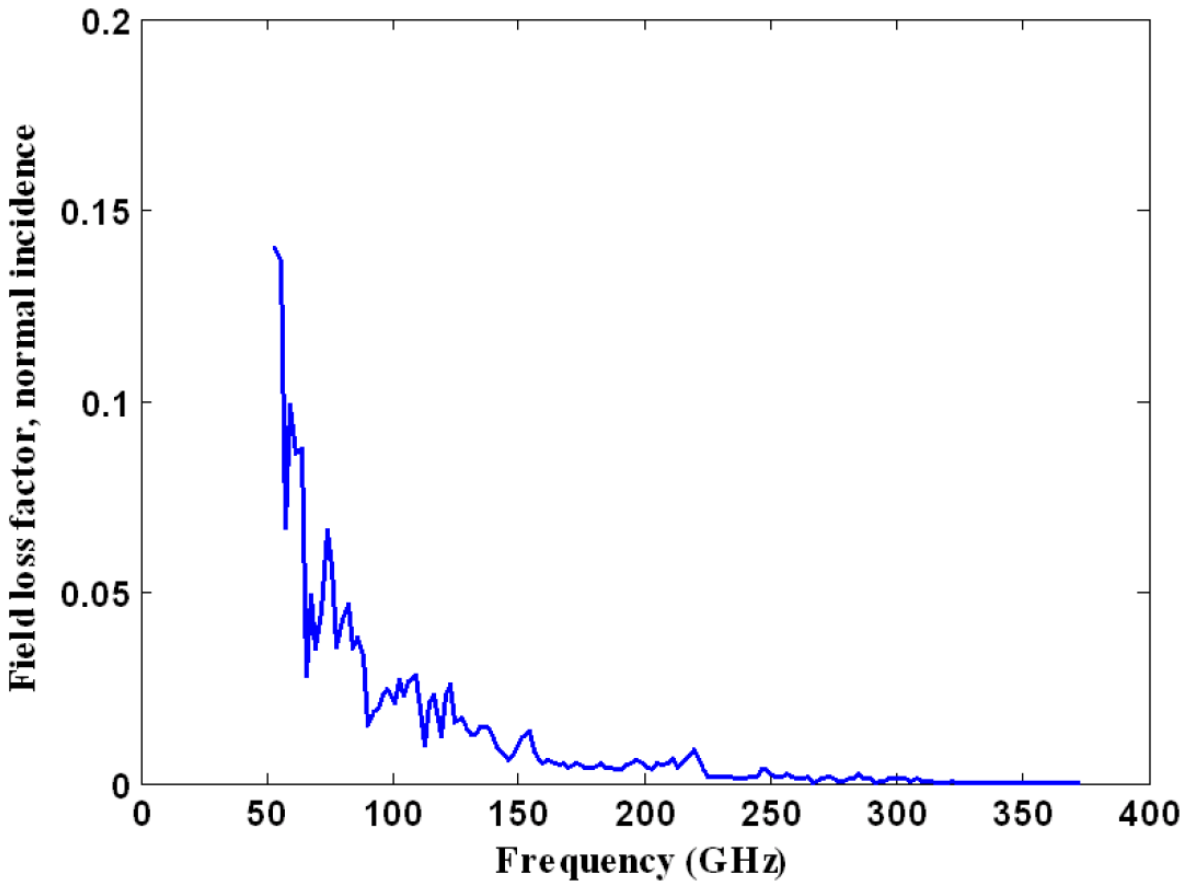

- Loss factor calculated with extracted n'' and z
- Higher order signal < 10% of last order signal magnitude for ~ 60GHz and up
- Verified extraction algorithms

Characterization of SWNT Thin Film on Substrates

Consider CNT layer as a boundary providing surface current

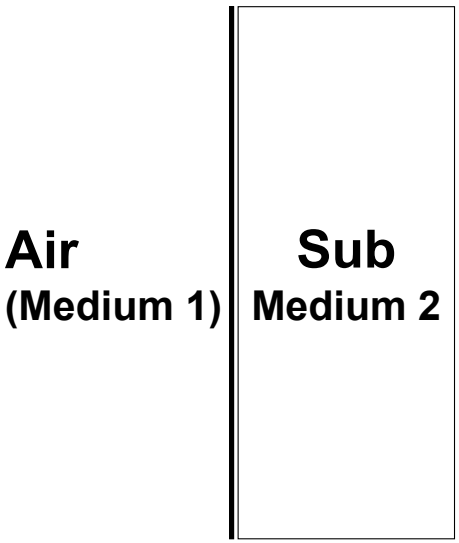

Reflection coeff: $\Gamma = \dfrac{Y_- - \sigma_s}{Y_+ + \sigma_s}$ ← Surface Conductivity

Transmission coeff: $T = \dfrac{2Y_1}{Y_+ + \sigma_s}$

With $Y_\pm = Y_1 \pm Y_2, Y = \dfrac{1}{Z} = \dfrac{n}{Z_0}$

SWNT Thin Film: ~ 300 nm thickness

3.2mm Pyrex glass

3.2mm thin window glass ← Thick substrate necessary to avoid multiple reflections

5mm thick window glass

Characterization of SWNT Thin Film on Substrates

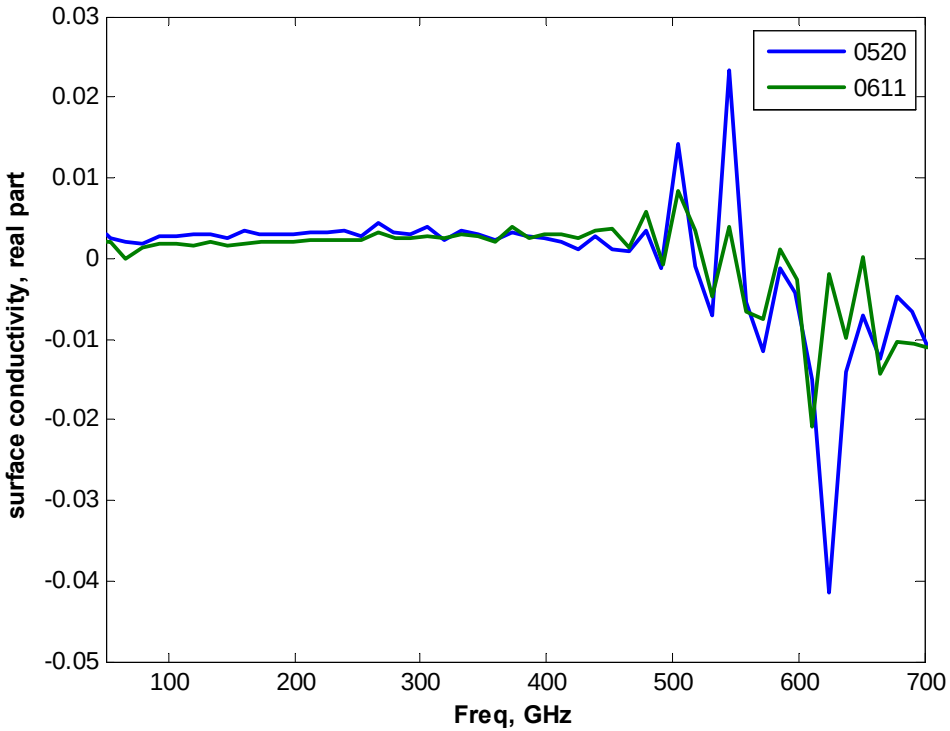

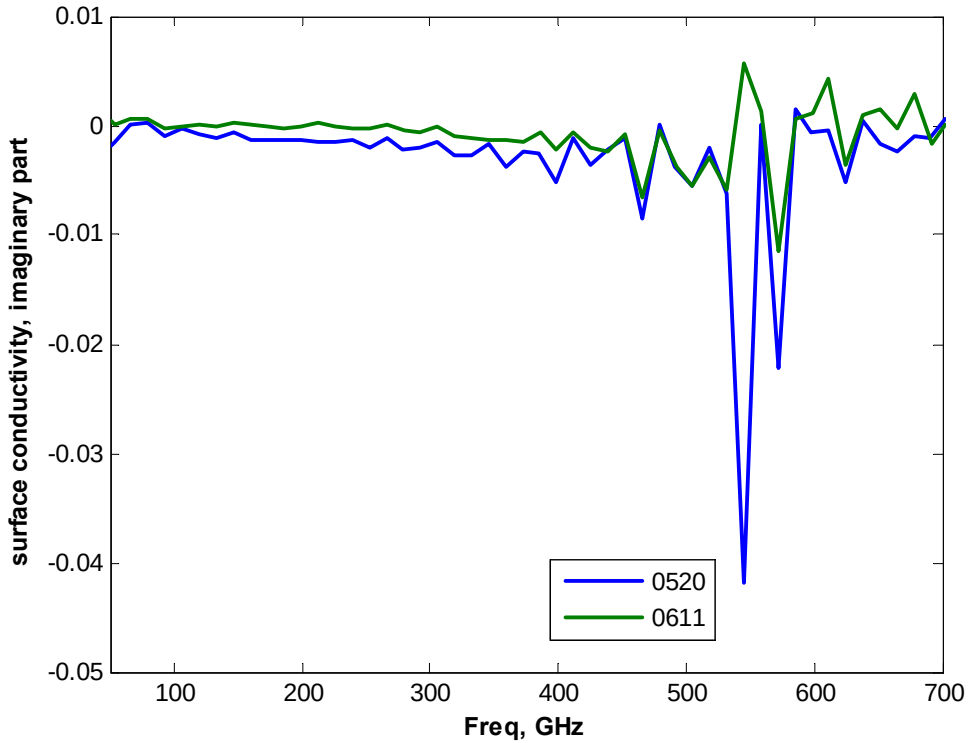

- More accurate real conductivity
- Measured surface conductivity
  - $\sigma * t = 0.015$ S (THz) and 0.0023 S (DC 4-point measurement)
  - $\sigma \sim 10^5$ Simens
- Peaks measured in conductivity
  - Systematic error / plasmonic resonances?
  - More study is under way

Under Study – Single Tube Measurement

Fabricate Grids on Insulating Substrate

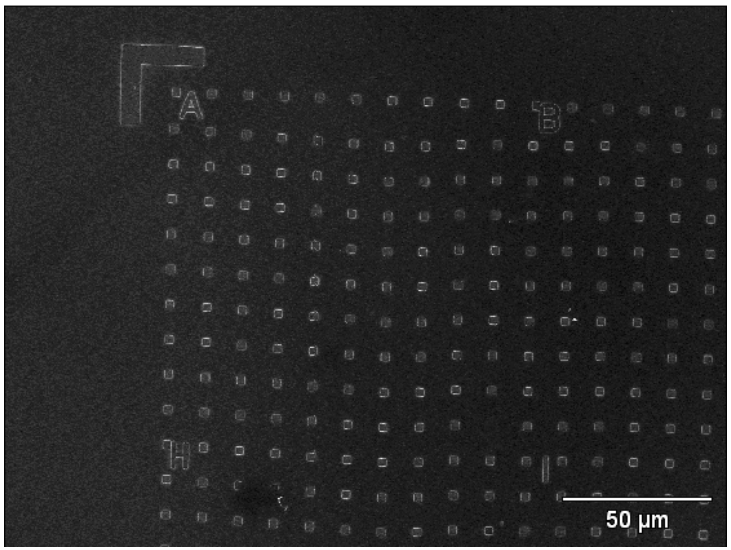

Disperse CNT and Locate Using AFM

EBL Fabrication of Designed Test Fixture

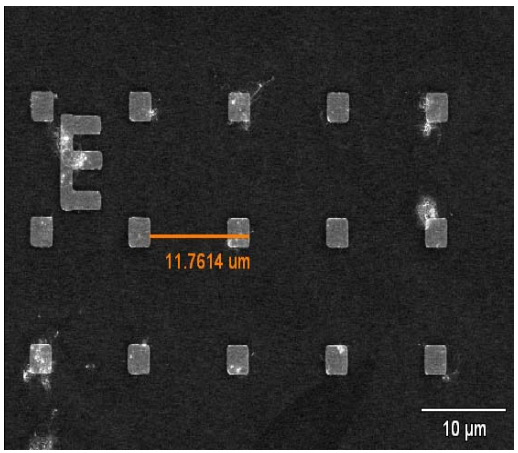

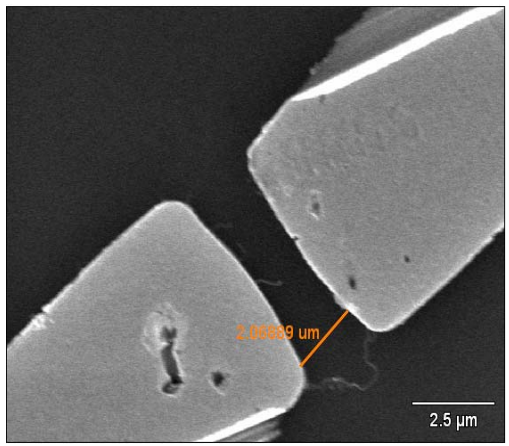

Microwave Property Probing and Extraction

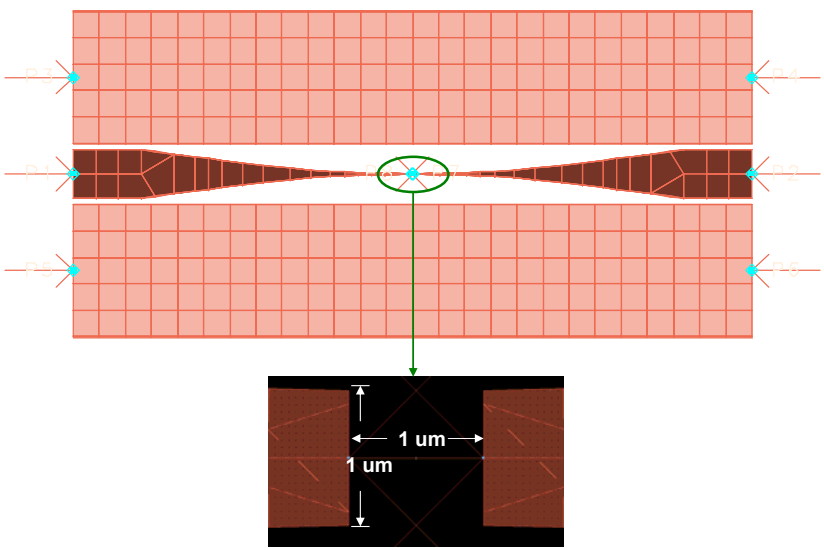

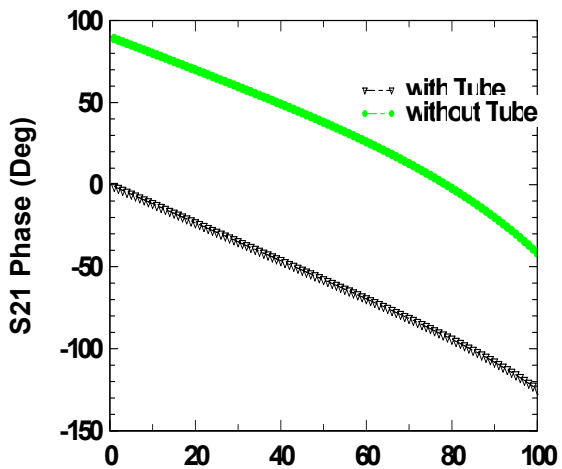

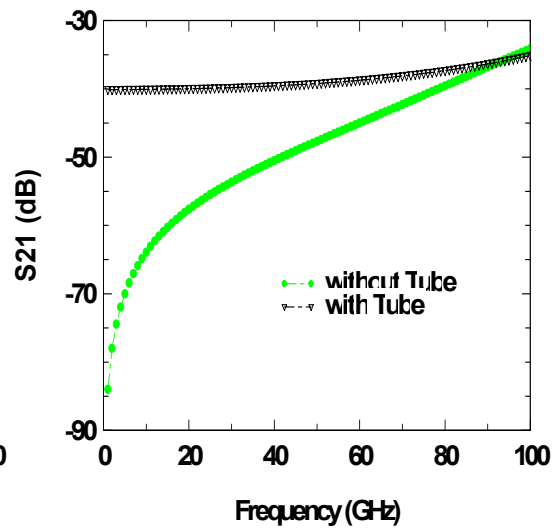

Conclusions

- Carbon nanotube maybe useful for high frequency applications
- Bulk (paper / thin film) materials characterized (8 – 400 GHz)
- Intrinsic material properties (permittivity & permeability) extracted
- Microwave & THz data are consistent
- Drude-Lorentz model fits measured permittivity
- Correlation of single tube and ensemble results under way